IOP PUBLISHING JOURNAL OF PHYSICS D: APPLIED PHYSICS

J. Phys. D: Appl. Phys. **43** (2010) 335103 (6pp) doi:10.1088/0022-3727/43/33/335103

J–V characteristics of dark and illuminated classical and inverted organic solar cells based on the CuPc/C_{60} heterojunction

M Morsli[1], L Cattin[2], J C Bernède[1], P Kumar[3] and S Chand[3]

[1] Université de Nantes, Nantes Atlantique Universités, LAMP, EA 3825, Faculté des Sciences et des Techniques, 2 rue de la Houssinière, BP 92208, Nantes, F-44000 France
[2] Université de Nantes, Nantes Atlantique Universités, Institut Jean Rouxel (IMN), Faculté des Sciences et des Techniques, 2 rue de la Houssinière, BP 92208, Nantes, F-44000 France
[3] Centre for Electronic Organic, National Physical Laboratory, Dr K.S. Krishnan Road, Pusa, New Delhi-110012, India

Received 6 April 2010, in final form 2 July 2010
Published 5 August 2010
Online at stacks.iop.org/JPhysD/43/335103

Abstract
A comparison of the performances of classical and inverted organic solar cells based on the junction copper phthalocyanine/fullerene (CuPc/C_{60}) shows that the former devices give the best efficiency. The transport properties of charge carriers in the organic material and the interface properties have been investigated using a mathematical simulation taking into account the effect of bulk and interface properties. Good agreement between experimental and calculated values can be achieved using different parameter values following the type of solar cells. In classical solar cells, the current is space charge limited, while there is no barrier at the contact electrode/organic material. In the case of inverted solar cells it is necessary to introduce a barrier contact at these interfaces to achieve a good fit between experimental and theoretical values. Therefore, the lower efficiency of the inverted solar cells is due to the barrier contact at the interface and smaller electrode work function difference.

1. Introduction

During the last 15 years the interest in organic solar cells has been continually growing [1]. A limiting factor affecting power conversion efficiency is the exciton diffusion length that is small prior to recombination. A typical exciton diffusion length is in the range of 10 nm. The film thickness should be higher than 100 nm in order to absorb most of the light. This difficulty has been overcome by using the concept of bulk heterojunction. This bulk heterojunction is obtained by blending an electron donor (D) and an electron acceptor (A). Blend cells exhibit a large interface area and most excitons reach the D/A interface. Although efficiency higher than 6% has been attained with P3HT : PCBM bulk heterojunctions, the morphology of the blend is difficult to control. Therefore, a possible way to control and stabilize the structure is to deposit the organic materials onto a well-structured anode such as ZnO nanorods [10]. Another way consists in the growth of tandem solar cells [2, 3].

The fundamental processes involved in efficient organic solar cells are (a) absorption of light, (b) creation and separation of the charge carriers at the D/A interfaces and (c) transport of these charges through the bulk of the device from the creation site to the appropriate collecting electrode. Therefore, first, the absorption spectrum of at least one of the organic materials should correspond, as nearly as possible, to the solar spectrum.

After creation, the pair of carriers should be separated. The separation takes place at the D/A interfaces. To achieve that goal, two configurations have been used, simple bilayer devices and bulk heterojunctions. An organic double layer solar cell contains an electron rich (electron donor, ED) and an electron deficient (electron acceptor, EA) layer. In a bulk heterojunction, both donor and acceptor are also present but

the ED/EA interfaces are distributed in the whole bulk of the sample.

In the case of a multi-layer thin film heterojunction the introduction of an electron blocking layer [4] between the cathode and the acceptor material allows achievement of good efficiencies. In these devices, transparent conductive oxide (TCO) coated substrates are usually used as the transparent anode, while the cathode is an aluminium evaporated film.

Another possibility is the use of inverted solar cells. In that case the TCO is used as the cathode, while a metallic electrode, with high work function, is used as the anode.

The classical multi-heterojunction structures are usually based on ITO/ABL/CuPc/C_{60}/CBL/Al devices where CuPc is the copper phthalocyanine, C_{60} is the fullerene, while ABL and CBL are the anode buffer layer and the cathode buffer layer, respectively. The buffer layers (ABL and CBL) are necessary in view of the difficulties in organic optoelectronic devices of the charge carrier transport between the organic materials and the electrodes.

In the case of the anode/electron donor contact, a common solution is to introduce a thin ABL, which adjusts the electronic behaviour of the adjacent materials. We have shown that an ultra-thin metal film or a thin oxide film deposited onto the conductive substrate, whatever TCO, can be used to improve the interface TCO/donor and therefore the devices' performance [5–7]. Indeed, Au and/or MoO_3 allow achievement of this goal [4], by simple vacuum deposition of an ultra-thin (0.5 nm) gold film or of a thin (3.5 ± 1 nm) MoO_3 film. Therefore, we have used Au as the ABL in classical solar cells, while MoO_3 of the MoO_3/Ag/MoO_3 can also be used as the ABL in classical as well as inverted solar cells. As a matter of fact, we have shown that MoO_3/Ag/MoO_3 can be an efficient transparent and conductive anode in organic solar cells [8]. There is a threshold silver thickness value, 10 nm, where the structures commute from an insulating state to a conductive state. We attribute this commutation to the percolation of the silver conducting path. The transmittance of the films increases when the silver thickness increases from 8 to 10 nm, while a further increase induces transmittance decrease. Such an effect is attributed to surface plasmon resonance. The structure with the best factor of merit is obtained when the silver thickness is 10 nm. Therefore, these structures can be used as anodes in classical and inverted organic solar cells.

In this paper, both classical and inverted solar cells have been studied.

The CBL is a large band gap material, such as bathocuproine (BCP) [9] or aluminium tris(8-hydroxyquinoline) (Alq_3) [11, 12]; it is called the exciton blocking layer (EBL). The EBL not only blocks the excitons far from the cathode, where they can be quenched, but also prevents the electron acceptor film from damage during cathode deposition. It should be transparent to the solar spectrum to act as a spacer between the photoactive region and the metallic cathode. It must, also, transport electrons to avoid high series resistance.

If the classical devices described above have given the best performance, development of inverted solar cells could allow more flexibility on designing tandem structures,

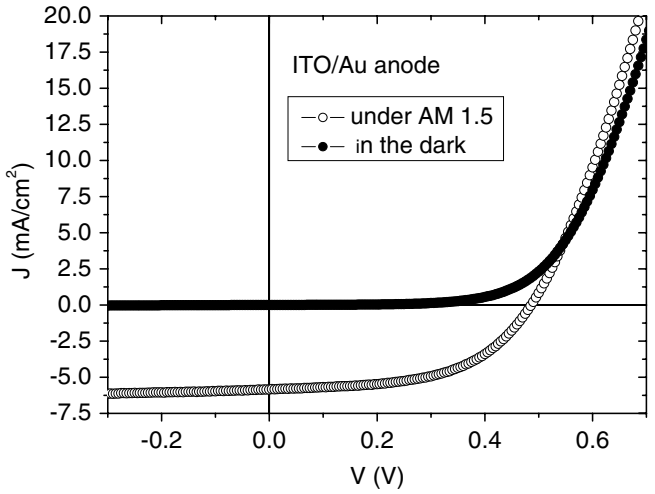

Figure 1. Typical J–V characteristics of glass/ITO(80 nm)/Au(0.5 nm)/CuPc(35 nm)/C_{60}(40 nm)/Alq_3(9 nm)/Al(100 nm) structure, in the dark (full symbol) and under illumination of AM1.5 solar simulation (100 mW cm^{-2}) (open symbol).

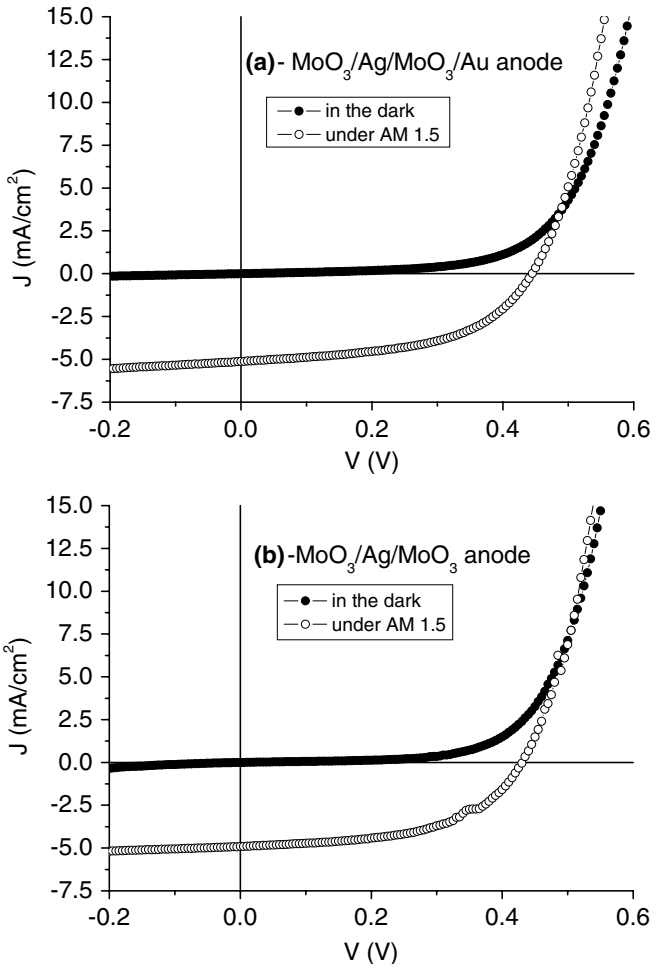

Figure 2. Typical J–V characteristics, in the dark (full symbol) and under illumination of AM1.5 solar simulation (100 mW cm^{-2}) (open symbol), of (*a*) glass/MoO_3/Ag/MoO_3/Au(0.5 nm)/CuPc(35 nm)/C_{60}(40 nm)/Alq_3(9 nm)/Al(100 nm) structure, (*b*) glass/MoO_3/Ag/MoO_3/CuPc(35 nm)/C_{60}(40 nm)/Alq_3(9 nm)/Al(100 nm) structure.

which can be formed using a semitransparent cathode. The structure of the inverted solar cells studied in this work is ITO/CBL/C_{60}/CuPc/MoO_3/Ag/MoO_3. The MoO_3/Ag/MoO_3 is used as the anode, while the first MoO_3 layer of this structure is also the ABL.

Up to now, the inverted organic solar cells studied are usually based on bulk heterojunctions [13, 14], while not many works have been devoted to inverted multi-heterojunction PV cells. The inverted bulk heterojunction structure has been highly successful and represents the device case that can be manufactured [15, 16]. The challenge to reversing the layer sequence of multi-heterojunction PV cells is achieving cathode and anode ohmic contacts.

In this work we study the (J–V) characteristics of classical and inverted OPV cells based on the CuPc/C_{60} couple.

2. Experimental

The glass substrates coated by an ITO thin film were provided by the SOLEMS. Other materials (Au, Ag, MoO_3, CuPc, C_{60} and Alq_3) were provided by Aldrich.

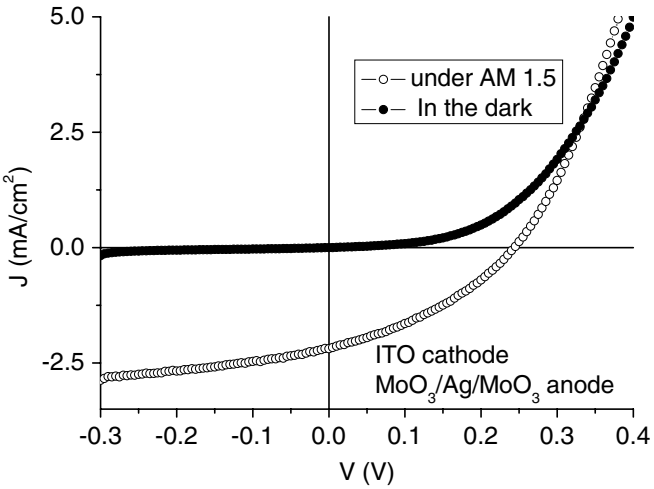

Figure 3. Typical J–V characteristics of glass/ ITO/Alq_3/C_{60}/CuPc/ MoO_3/Ag/ MoO_3 structure, in the dark (full symbol) and under illumination of AM1.5 solar simulation (100 mW cm^{-2}) (open symbol).

2.1. Classical organic solar cells

In the case of classical cells, an ultra-thin gold film (thickness $t = 0.5$ nm), used as the ABL, was deposited onto some ITO anodes to increase the cells' performance [5, 6, 17].

The organic solar cells' structure is anode/organic electron donor/organic electron acceptor/organic buffer layer/aluminium. The anode is ITO/Au (0.5 nm), MoO_3/Ag/ MoO_3 and MoO_3/Ag/MoO_3/Au. The electron donor is CuPc, the electron acceptor is C_{60}, the buffer layer is Alq_3 [11, 12]. All the organic cells were prevented from air contamination by an amorphous selenium thin film [7, 8, 12]. The deposition conditions have been described earlier [17]. Finally, the structures used were

glass/anode/CuPc(35 nm)/C_{60}(40 nm)/Alq_3(9 nm)/ Al(100 nm).
Anode = ITO/Au (0.5 nm), MoO_3/Ag/MoO_3 or MoO_3/Ag/ MoO_3/Au.

2.2. Inverted organic solar cells

In the case of inverted cells, the thin film sequence is as follows: ITO/Alq_3(9 nm)/C_{60}(40 nm)/CuPc (35 nm)/MoO_3/Ag/ MoO_3. The CBL in this case also is Alq_3. The experimental conditions for thin film deposition are the same as those used for classical solar cells.

Electrical characterizations were performed with an automated I–V tester, in the dark and under sun global AM1.5 simulated solar illumination. The performance of the photovoltaic cells was measured using a calibrated solar simulator (Oriel 300W) at 100 mW cm^{-2} light intensity adjusted with a PV reference cell (0.5 cm^2 CIGS solar cell, calibrated at NREL, US). The measurements were performed in ambient atmosphere. All devices were illuminated through ITO electrodes.

3. Experimental results and discussion

Typical J–V characteristics, in the dark and under one sun global AM1.5 simulated solar illumination, are presented in figures 1–3. The open circuit voltage (V_{oc}), the short circuit current density (J_{sc}), the fill factor (FF) and the power cells' conversion efficiency (η) are presented in table 1. As expected,

Table 1. Photovoltaic performance data and parasitic resistances under AM1.5 conditions of the devices of figures 1–3.

Sample	J_{sc} (mA/cm^2)	V_{oc} (V)	FF (%)	η (%)	R_s	R_{sh}
Classical solar cells						
ITO/Au/CuPc(35 nm)/C_{60}/Alq_3/Al	5.84	0.49	53.9	1.53	174	8190
ITO/Au/CuPc(40 nm)/C_{60}/Alq_3/Al	5.08	0.48	52.9	1.30	216	9684
MoO_3/Ag/MoO_3/CuPc(35 nm)/C_{60}/Alq_3/Al	4.90	0.430	52	1.15	143	6315
MoO_3/Ag/MoO_3/Au/CuPc(35 nm)/C_{60}/Alq_3/Al	5.12	0.444	52	1.19	144	4050
Inverted solar cells						
ITO/Alq_3/C_{60}/CuPc(35 nm)/MoO_3/Ag/MoO_3. Surface area 0.15 cm^2	2.45	0.27	36.8	0.24	495	2535
ITO/Alq_3/C_{60}/CuPc(35 nm)/MoO_3/Ag/MoO_3. Surface area 0.10 cm^2	2.91	0.24	35.3	0.25	460	2780

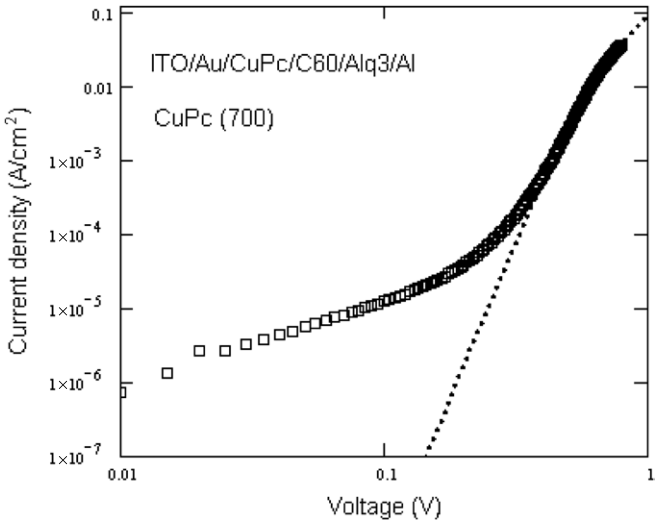

Figure 4. Calculated (· · · · · ·) and experimental (□) J–V characteristics of glass/ITO(80 nm)/Au(0.5 nm)/CuPc(35 nm)/C_{60}(40 nm)/Alq_3(9 nm)/Al(100 nm) organic solar cell.

the classical organic solar cell structures give better results, while the inverted organic solar cells give promising but lower efficiencies. It can be seen that the best results are obtained with ITO/Au. All the current densities are given for an area of 10 mm^2. More precisely, it can be seen in table 1 that the short circuit current density and the FFs of the inverted solar cells are smaller than those of the classical solar cells. Also the open circuit voltage of the inverted cells is only half of that of the classical cells.

The slopes at the short circuit point and at the open circuit voltage are the inverse values of the shunt resistance (R_{sh}) and the series resistance (R_s) of the equivalent circuit scheme of a solar cell, respectively [18]. It can be immediately seen from table 1 that the best cells correspond to the smaller R_s and higher R_{sh}.

In such devices, the process of carrier collection is one of the main factors which controls the electrical characteristics and the efficiency of the devices. Therefore, electrode modification can lead to good or bad performance solar cells.

In order to explain the different types of cell behaviour, the modelling of J–V characteristics could be helpful in understanding and optimizing organic solar cells by providing a quantitative estimation for losses in the cells.

The current–voltage (I–V) characteristics of metal/polymer/metal devices are controlled by two basic processes: injection of charge carriers from the electrodes into the organic material and vice versa and/or transport of charge in the bulk of the organic film. The current in the device is determined by the less effective mechanism, which limits charge carrier flow. It is crucial for the understanding and optimization of organic devices to obtain an answer to the question of whether their characteristics are controlled by interface exchange or bulk transport.

So far, different descriptions of the J–V behaviour of organic solar cells have been provided, using either Schottky barrier or space charge limited current (SCLC), but these

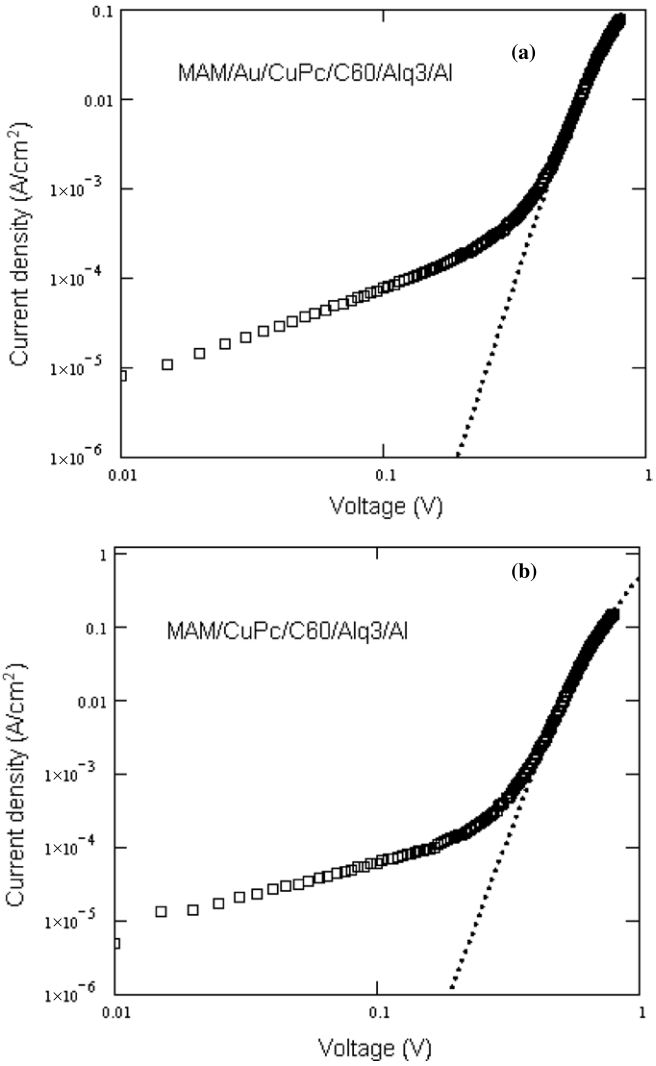

Figure 5. Calculated (· · · · · ·) and experimental (□) J–V characteristics of (*a*) glass/MoO_3/Ag/MoO_3/Au(0.5 nm)/CuPc(35 nm)/C_{60}(40 nm)/Alq_3(9 nm)/Al(100 nm) (*b*) glass/MoO_3/Ag/MoO_3//CuPc(35 nm)/C_{60}(40 nm)/Alq_3(9 nm)/Al(100 nm).

models were exclusive. Recently, a model which includes both injection and bulk transport properties has been proposed [19]. According to this model the current can even be SCLC if the injection barrier is not very high. This model explains the effect of injection barrier height on SCLC. Most of the organic semiconductors are disordered materials and possess traps. In that case the transport equations and Poisson's equations will, respectively, be written as

$$J = q\mu p(x)F(x) \tag{1}$$

and

$$\frac{\mathrm{d}F}{\mathrm{d}x} = q\frac{\{p(x) + p_t(x)\}}{\varepsilon\varepsilon_0}, \tag{2}$$

where q is the elementary charge, μ is the carrier mobility, $p(x)$ is the free carrier distribution, $p_t(x)$ is the trapped carrier distribution, $F(x)$ is the electric field distribution and ε, ε_0 are, respectively, the dielectric constant and permittivity of free space. Usually in most of the organic semiconductors

the traps are distributed exponentially in energy space and for exponential distribution of traps,

$$p_t(x) = H_b \left(\frac{p(x)}{N_v} \right)^{1/l}, \quad (3)$$

where H_b is the total trap density, N_v is the effective density of states and $l = T_c/T$, where T_c is the characteristic temperature of trap distribution and T is the absolute temperature. If $p(x)$ is less than $p_t(x)$, $p(x)$ can be ignored in equation (2) and equations (1)–(3) can be solved analytically to derive the J–V relation [20]. It is also shown that at high voltages $p(x)$ cannot be ignored compared with $p_t(x)$. In this case, from equations (1) and (2) we get

$$\int_0^d \mathrm{d}x = \frac{\varepsilon\varepsilon_0}{q} \int_{F(0)}^{F(d)} \frac{\mathrm{d}F}{\frac{J}{q\mu F} + H_b \left(\frac{J}{q\mu N_v F} \right)^{1/l}}. \quad (4)$$

The analytical solution of equation (4) is very difficult, therefore the solution is obtained by numerical calculations. The way to calculate the J–V characteristics in this case has been discussed by some of the authors of this paper in [16].

We have compared our experimental data with the calculated characteristics using equation (4). The experimental data have been observed to be in good agreement with the calculated characteristics using equation (4). The experimental data were also compared with other models, for example Richardson–Schottky thermionic emission, Fowler–Nordheim tunnelling, thermal assisted tunnelling and mobility model [21, 22]. The experimental data did not show any agreement with any of these models.

The J–V characteristics were calculated using equation (4) with the following values of parameters: $\varepsilon = 3$, $d = 75$ nm, $N_v = 10^{19}$ cm^{-3} and $T = 300$ K. From the curves log J–log V, we observe in figures 4–6 that below a critical voltage the current density varies linearly on the voltage, which corresponds to an ohmic regime. For voltage above the critical voltage, the current density strongly increases which is characteristic for SCLC. The transition between the two different regimes is sharp for trap levels located at a single energy [23]. The gradual transition visible in the figures points to a distribution of trap-level energies.

It can be seen in figures 4–6 that at low voltages curves show ohmic behaviour which can be attributed to background doping and thermally generated charge carriers. At higher voltages the experimental data (symbols) show good agreement with the numerically calculated curves (dashed curves) for SCLC with exponentially distributed traps in energy and space. The parameter values calculated are given in table 2. The main information given by table 2 is that to achieve good agreement between experimental and calculated J–V characteristics the value of the barrier height should not be zero only in the case of inverted solar cells. About T_c, values of the same order of magnitude have already been observed in some other organic semiconductors as well [24, 25].

As shown above, the low efficiency in inverted solar cells can be attributed to the low values of V_{oc}, FF and J_{sc}. From the results summarized in table 2 it can be said that the low FF and J_{sc} are due to the presence of a barrier at the contact ITO/electron acceptor, since it has already been shown that the interfaces CuPc/MAM and CuPc/Au/MAM are good quality contacts [8].

As usual, the low V_{oc} value corresponds to low shunt resistance. It may be attributed to the fact that in inverted solar cells the top anode, MoO_3/Ag/MoO_3, may diffuse much more in CuPC than Al into C_{60} in the classical case, since there is no protective interlayer in the former case while there is an Alq_3 intermediate layer in the latter case. The diffusion may in turn result in conducting shorts in the active layer.

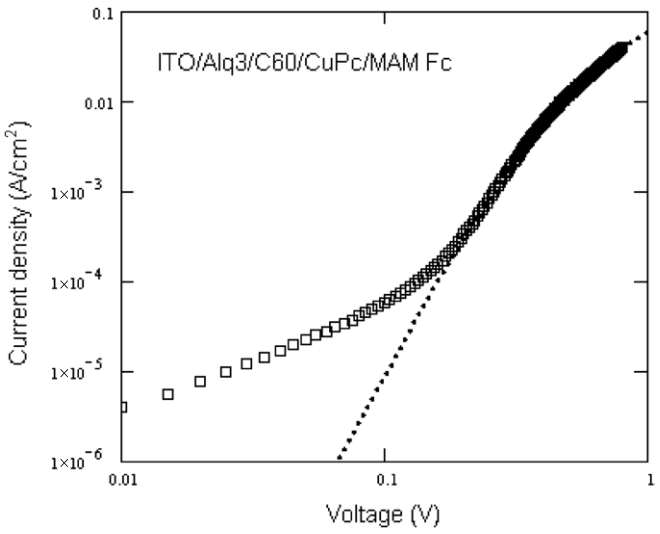

Figure 6. Calculated (· · · · · ·) and experimental (□) J–V characteristics of glass/ITO/Alq_3/C_{60}/CuPc/ MoO_3/Ag/ MoO_3.

Table 2. Parameters values calculated using equation (4).

Sample	μ (cm^2 V^{-1} s^{-1})	T_c (K)	H_b (cm^{-3})	ϕ (eV)
Classical organic solar cells				
ITO/Au/CuPc(35 nm)/C_{60}/Alq_3/Al	4.8×10^{-4}	2200	1.0×10^{17}	0
ITO/Au/CuPc(40 nm)/C_{60}/Alq_3/Al	3.5×10^{-4}	1950	1.2×10^{17}	0
MoO_3/Ag/MoO_3/Au/CuPc(35 nm)/C_{60}/Alq_3/Al	1.8×10^{-3}	2400	1.0×10^{17}	0
MoO_3/Ag/MoO_3/CuPc(35 nm)/C_{60}/Alq_3/Al	2.5×10^{-3}	2550	9.0×10^{16}	0
Inverted organic solar cells				
ITO/Alq_3/C_{60}/CuPc(35 nm)/ MoO_3/Ag/MoO_3. Surface area 0.15 cm^2	4×10^{-4}	775	5×10^{17}	0.12

Moreover, it is generally admitted that the V_{oc} increases with the work function difference of the electrodes [26]. In the case of classical solar cells the work function difference, taking into account the buffer layers, is $\Phi_{Au}-\Phi_{Al}$ or $\Phi_{MoO_3}-\Phi_{Al}$ that is to say it is around 0.9 eV. For reversed solar cells the same estimation gives $\Phi_{ITO}-\Phi_{MoO_3}$, that is to say around 0.6 eV. Such an electrode work function difference can explain the smaller value of V_{oc} of inverted solar cells.

4. Conclusion

In conclusion, the efficiency difference between classical and inverted multilayer organic solar cells has been justified using a mathematical simulation on charge carrier transport in organic solar cells. The lower efficiency of inverted solar cells can be attributed to the presence of a barrier at the interface cathode/electron acceptor and to its smaller electrode work function difference.

References

[1] Cai W, Gong X and Cao Y 2010 *Sol. Energy Mater. Sol. Cells* **94** 114

[2] Ameri T, Dennler G, Lungenschmied C and Brebec C J 2009 *Energy Environ. Sci.* **2** 347

[3] Helgersen M, Sendergaard R and Krebs F C 2010 *J. Mater. Chem.* **20** 36

[4] Chan M Y, Lai S L, Fung M K, Lee C S and Lee S T 2007 *Appl. Phys. Lett.* **90** 023504

[5] Bernède J C, Berredjem Y, Cattin L and Morsli M 2008 *Appl. Phys. Lett.* **92** 083304

[6] Bernède J C, Cattin L, Morsli M and Berredjem Y 2008 *Sol. Energy Mater. Sol. Cells* **92** 1508

[7] Cattin L, Dahou F, Lare Y, Morsli M, Tricot R, Jondo K, Khelil A, Napo K and Bernède J C 2009 *J. Appl. Phys.* **105** 034507

[8] Cattin L, Morsli M, Dahou F, Yapi Abbe S, Khelil A and Bernède J C 2010 *Thin Solid Films* **518** 4560

[9] Peumans P, Bulovic V and Forrest S R 2000 *Appl. Phys. Lett.* **76** 3855

[10] Gonzalez-Valls I and Lira-Cantu M 2009 *Energy Environ. Sci.* **2** 19

[11] Song Q L, Li F Y, Yang H, Wu H R, Wang X Z, Zhou W, Zhao J M, Ding X M, Huang C H and Hou X Y 2005 *Chem. Phys. Lett.* **416** 42

[12] Berredjem Y, Karst N, Boulmokh A, Gheid A H, Drici A and Bernède J C 2007 *Eur. Phys. J.: Appl. Phys.* **40** 163

[13] Meiss J, Allinger N, Riede M K and Leo K 2008 *Appl. Phys. Lett.* **93** 103311

[14] Hau S K, Yip H-L, Ma H and Jen A K-Y 2008 *Appl. Phys. Lett.* **93** 233304

[15] Krebs C K, Nielsen T D, Fyenbo J, Wadstrom M and Pedersen M S 2010 *Energy Environ. Sci.* **3** 512

[16] Krebs C K, Gevorgyan S A and Alstrup J 2009 *J. Mater. Chem.* **19** 5442

[17] Kouskoussa B, Morsli M, Benchouk K, Louarn G, Cattin L, Khelil A and Bernède J C 2009 *Phys. Status Solidi* a **206** 311

[18] Brousse B, Ratier B and Moliton A 2004 *Synth. Met.* **147** 293

[19] Kumar P, Jain S C, Kumar V, Misra A, Chand S and Kamalasanan M N 2007 *Synth. Met.* **157** 905

[20] Jain S C, Kapoor A K, Geens W, Poortmans J and Mertens R 2002 *J. Appl. Phys.* **92** 3752

[21] Tanase C, Blom P W M and de Leeuw D M 2004 *Phys. Rev.* **B 70** 193202

[22] Torricelli F, Zappa D and Colalongo L 2010 *Appl. Phys. Lett.* **96** 113304

[23] Blom P W M, de Jong M J M and Vleggar J J M 1996 *Appl. Phys. Lett.* **68** 3308

[24] Kapoor A K, Jain S C, Poortmans J, Kumar V and Mertens R 2002 *J. Appl. Phys.* **92** 3835

[25] Kumar P, Misra A, Kamalasanan M N, Jain S C, Srivastava R and Kumar V 2006 *Japan. J. Appl. Phys.* **45** 7621

[26] Zhou Y, Li F, Barrau S, Tian W, Inganäs O and Zhang F 2009 *Sol. Energy Mater. Sol. Cells* **93** 497